Dynamic of Land Use Land Cover and its Impact on Land Surface Temperature (LST) Using GIS: A Study of District Mardan, Pakistan

Zain Sultan, Muhammad Awais Khan, Zahid Khan, Muhammad Sudais, Nigar Khan, Aizaz Ullah, Muddasir Ali
Department of Geography & Geomatics (GIS/RS), University of Peshawar, Pakistan
*Correspondence: zainsultan0334@gmail.com

Citation | Sultan. Z, Khan. M. A, Khan. Z, Sudais. M, Khan. N, Ullah. A, Ali. M, "Dynamic of Land Use Land Cover and its Impact on Land Surface Temperature (LST) Using GIS: A Study of District Mardan, Pakistan", IJIST, Special Issue pp 472-488, June 2024
Received| June 12, 2024 **Revised|** June 17, 2024 **Accepted|** June 21, 2024 **Published|** June 29, 2024.

Rapid population growth is a global issue that alters landscapes and affects environmental conditions. This study aims to assess the effects of urbanization on Land Use Land Cover (LULC) changes and their impact on Land Surface Temperature (LST) in District Mardan from 2002 to 2022. By combining remote sensing data on LULC changes with LST measurements, researchers can analyze the relationship between these variables. This analysis sheds light on how LULC changes affect local climate patterns, urban heat island effects, and the overall thermal environment. Data preprocessing was done using ArcGIS 10.8 software. After preprocessing, a supervised classification scheme was applied for 2002 and 2022, using the maximum likelihood algorithm to identify LULC changes. In 2002, the built-up area covered 165.47 km², which increased to 266.70 km² by 2022. Vegetation covers gradually declined over the same period, with a notable shift from vegetation to built-up areas. The study revealed significant changes in District Mardan, including population growth, urban expansion, and infrastructure development. These changes were influenced by various factors, including land cover types. The results of this study can be useful for regional and urban planning, as well as for managing agricultural practices in the future.

Keywords: LULC; GIS; Land Surface Temperature; Urban Expansion.

Introduction:

The modification of Earth's terrestrial surface by human activities is commonly referred to as land use land cover (LULC) change worldwide [1]. LULC is primarily influenced by factors such as ecological conditions, geological structure, altitude, and slope, along with socio-economic, technological, and institutional factors that significantly affect land-use patterns in a given area [2]. The term LULC encompasses how land is utilized for purposes such as agriculture, conservation, urban development, recreation, wildlife habitats, and more, reflecting the outcomes of human-environment interactions influenced by socioeconomic factors and climate change processes [3]. Changes in LULC play a critical role in altering environmental conditions both locally and globally [4]. These changes are driven by human activities, including rapid urbanization and population growth, leading to significant transformations in the Earth's surface [5].

Cities have existed for thousands of years, dating back to the first human settlements in Mesopotamia between 4000 BC and 3000 BC. Today, more than half of the global population resides in urban areas, with humans evolving into city-dwelling "metro sapiens" in pursuit of sustainability [6]. It is well-documented that urbanization significantly impacts local weather and climate. Urban climate studies have long focused on the difference in air temperatures between cities and their rural surroundings, a phenomenon known as the urban heat island (UHI) effect [6]. The primary cause of UHI is the alteration of land surfaces, and according to Ackerman, urban areas experience temperatures 2–5 degrees higher than those of rural areas [7]. The intensity of land surface temperature is closely linked to LULC changes, such as the replacement of vegetative cover with buildings, paved surfaces, bare ground, and water bodies [8]. The loss of vegetation and its replacement with built-up infrastructure contributes to the UHI effect, where urban areas experience higher temperatures compared to rural regions, negatively impacting the lives and daily activities of urban populations [9]. Studies have examined the relationship between LST patterns and land cover in places like Guangzhou and the urban clusters of the Zhejiang Delta in China, with satellite-derived radiant temperatures highlighting the surface temperature heat island phenomenon [10].

Objectives:

- To analyze the land use and land cover of the study area and track its changes from 2002 to 2022.
- To investigate the spatial distribution and variations in Land Surface Temperature (LST) across the study area and assess the impact of LULC changes on LST.

Novelty Statement:

The title of this study introduces a novel concept, exploring how LULC changes, driven by human activity, have occurred due to population growth in the study area from 1981 to 2023, as reported by the census. These LULC changes have impacted the Land Surface Temperature (LST) of the region. The primary goal of this research is to analyze the dynamics of LULC and identify the factors influencing LST.

Material and Methods:

Study Area:

The study area, Mardan District, is located in the Peshawar Valley, historically part of the Gandhara Kingdom. Until 1937, Mardan was part of Peshawar District but became an independent district that year. Mardan lies between latitudes 34° 04' 40" to 34° 31' 51" N and longitudes 71° 49' 05" to 72° 26' 04" E. It is bordered by Buner and Malakand districts to the north, Swabi and Buner districts to the east, Nowshera district to the south, and Charsadda and Malakand districts to the west, as shown in Figure 1. The total geographic area of Mardan District is 1,632 km². According to the 1998 census, the population was 1,460,100, which increased to 2,373,399 by the 2017 census and further to 2,744,898 according to the 2023 census [11][12]. The climate of the district is based on data from the nearby Risalpur station,

which shares similar topography. The average temperature is 22.2°C, and the annual precipitation averages 559 mm. Streams in the district generally flow from north to south, most draining into the Kabul River. The Kalpani stream, an important watercourse in the district, originates in Baizai and flows south to join the Kabul River. Key tributaries include Baghiari Khawar to the west, Muqam Khawar from Sudham Valley, and Naranji Khawar from the Narangi Hills [13]. The primary source of irrigation is the canal system. The upper Swat canal irrigates most of the district, while the lower Swat canal serves the southwestern areas. Other irrigation sources include tube wells and lift irrigation (GOP, 1998).

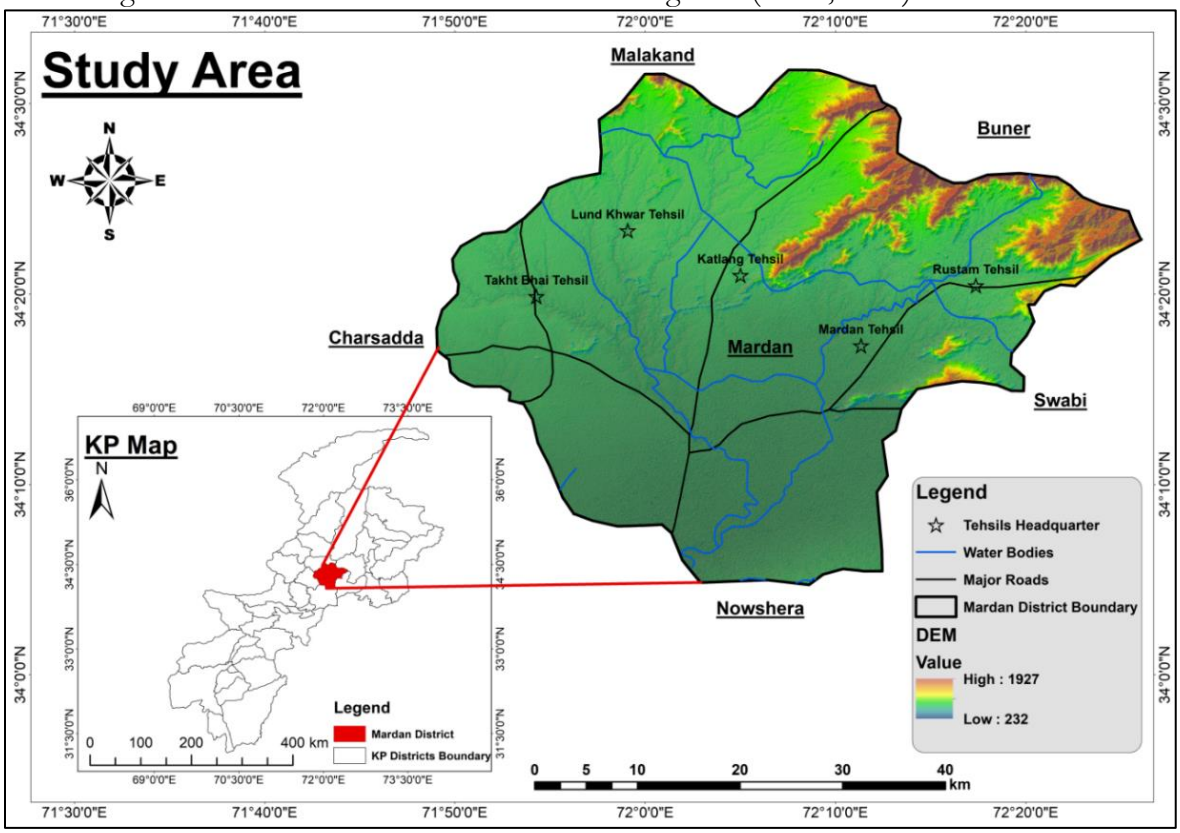

Figure 1: Location Map of the Study Area

Methodology and Analysis:

- The first step involves data acquisition, where satellite imagery from Landsat 7 and Landsat 8 is obtained from the USGS for LULC and LST analysis.
- The second step is correlating LST with spectral indices, such as NDVI, NDBI, NDWI, SAVI, and BI.
- In the third step, changes from the previous study year are extracted and analyzed through to the next study year.

Image Classification:

The maximum likelihood algorithm is a widely used method for classification in remote sensing. This method requires a signature file with a (.gsg) extension as input to perform probability-based classification. Maximum Likelihood Classification (MLC) was applied to modify and correlate each class signature [14]. The main objective of MLC is to classify raster data into distinct classes, resulting in a classified image that is automatically converted into a raster format within ArcMap.

Extraction of LST from Thermal Band:

LST (Land Surface Temperature) extraction involves converting sensor measurements into physical quantities. A sensor captures the intensity of electromagnetic radiation for each pixel as a digital number (DN), which must be converted into more meaningful real-world

units, such as radiance (Watts), reflectance, or brightness temperature. The following steps were used to extract LST from the thermal bands of Landsat imagery.

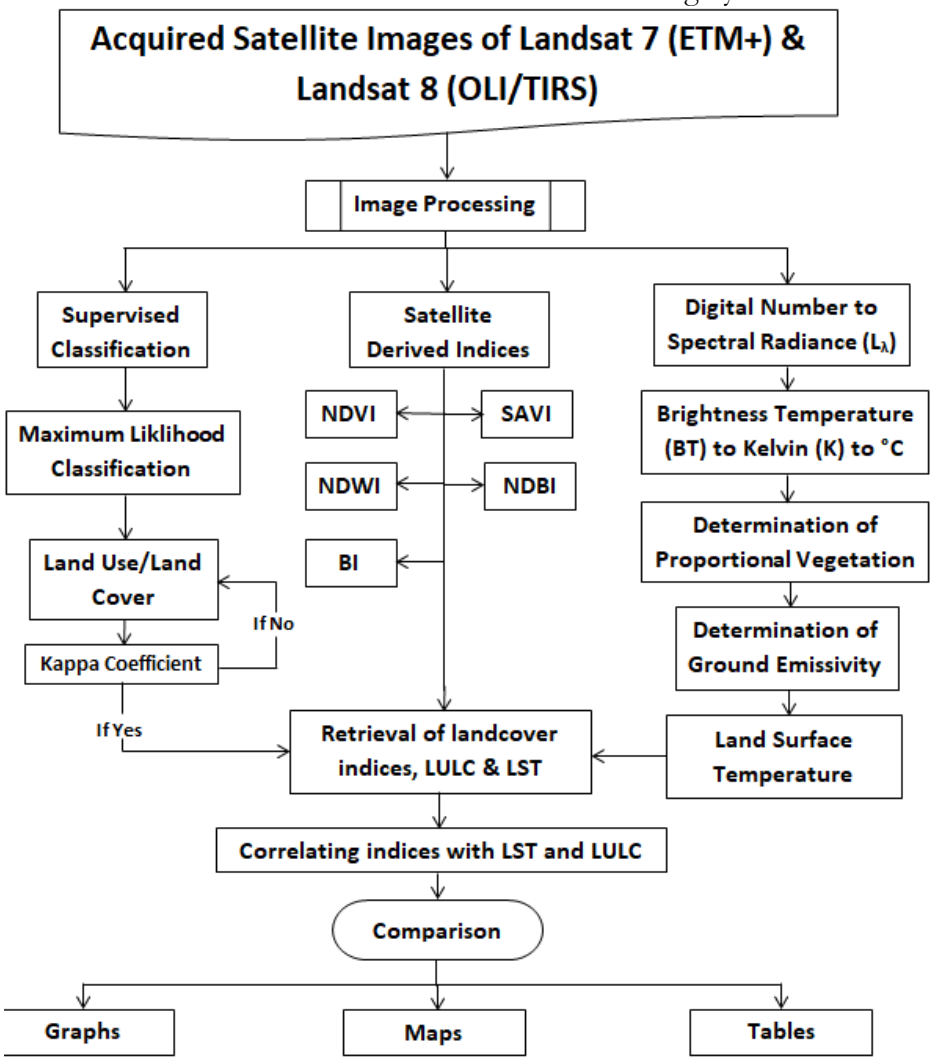

Figure 2: Flow Chart

Conversion of Digital Number (DN) to Spectral Radiance:

Any object with a temperature above absolute zero (K) emits thermal electromagnetic energy. Data captured by thermal sensors can be transformed into at-sensor radiance using radiance rescaling factors provided in the metadata file.

$$L_\lambda = M_L Q_{cal} + A_L \quad (1)$$

Lλ represents the Top of Atmosphere (TOA) spectral radiance, measured in Watts/ (m^2 * sr * μm). ML is the band-specific multiplicative rescaling factor obtained from the metadata (denoted as RADIANCE_MULT_BAND_x, where x refers to the band number). AL is the band-specific additive rescaling factor from the metadata (RADIANCE_ADD_BAND_x, where x indicates the band number). Q refers to the quantized and calibrated standard product pixel values (Digital Numbers, DN).

Conversion to At-Satellite Brightness Temperature:

The band data is then converted from spectral radiance to top-of-atmosphere (TOA) brightness temperature using the thermal constants provided in the metadata file, as shown in Equation 2.

$$Tb = K*2 / \ln (k\,1 / L\lambda + 1) \quad (2)$$

Here, T or BT represents the Top of Atmosphere (TOA) brightness temperature in Kelvin (K). Lλ denotes the TOA spectral radiance in Watts / (m^2 * sr * μm). K1 is the band-

specific thermal conversion constant from the metadata (K1_CONSTANT_BAND_x, where x is the thermal band number), and K2 is the band-specific thermal conversion constant from the metadata (K2_CONSTANT_BAND_x, where x is the thermal band number).

Land Surface Temperature:

Land surface temperature was retrieved using a single-channel algorithm, which utilizes a single thermal band from the dataset. Since the temperature obtained through this method is referenced to a blackbody, corrections for land surface emissivity are required. Emissivity can be derived from the normalized difference vegetation index (NDVI) [15]. The emissivity-corrected land surface temperature was calculated using the procedure proposed by Arties and Carnahan (1982), as detailed in Equation 3.

$$LST = Tb / [1 + \{(\lambda * Tb / \varrho) * \ln\epsilon\}] \quad (3)$$

Here, Tb represents the satellite brightness temperature, λ is the wavelength of emitted radiance, and p is calculated as \ (\frac {h \cdot c} {s} \) (1.438 × 10^{-2} m K), where \(h \) is Planck's constant (6.626 × 10^{-34} Js), \(s \) is the Boltzmann constant, and \(c \) is the speed of light (2.998 × 10^{8} m/s). Emissivity (e) is defined as the ratio of the energy radiated from a material's surface to that radiated from a blackbody (a perfect emitter) at the same temperature, wavelength, and viewing conditions. It will be calculated using the following equation:

$$LSE = 0.004 * PV + 0.986 \quad (4)$$

Where PV means proportion of vegetation and can be calculated using equation 5:

$$PV = \sqrt{(NDVI - NDVI_{min} / NDVI_{max} - NDVI_{min})}$$

Conversion of LST from Kelvin to Celsius:

The retrieved LST is in Kelvin, and it can be converted to Celsius by subtracting 273.15 from the Kelvin value. This conversion is carried out using Equation 5.

$$LST - 273.15 \quad (5)$$

Result and Discussion:

Spatio-Temporal LULC Trend:

Figures 3 and 4 illustrate how land use and land cover (LULC) in Mardan District changed from 2002 to 2022. Figure 3 shows significant changes in the built-up area in the city center in 2002, indicating the early stages of urban growth. By 2022, as depicted in Figure 4, there was a noticeable increase in the built-up area, primarily concentrated in the district center. This period also saw a low vegetation index, likely due to reduced rainfall. Smaller built-up areas began emerging throughout the region, suggesting irregular urban expansion [16]. The substantial increase in built-up areas can be attributed to numerous housing developments in Mardan and neighboring cities between 2002 and 2022. This rapid urbanization resulted in a significant decline in plant cover, underscoring the trade-off between urban expansion and green spaces.

A quantitative summary of the major LULC changes between 2002 and 2022, using the Maximum Likelihood Classification (MLC) algorithm, is provided in Table 1. The data reveals a significant increase in built-up areas, with notable changes in agricultural and vegetative fields and urban settings [17]. Specifically, the built-up area grew from 165.47 km² (10.10% of the total area) to 266.70 km² (16.28%). Concurrently, vegetation areas decreased, while bare terrain either remained stable or slightly increased. Water bodies expanded from 25.03 km² (1.53%) to 49.61 km² (3.03%), barren land increased from 518.60 km² (31.67%) to 528.46 km² (32.27%), and vegetative areas declined from 928.76 km² (56.70%) to 793.09 km² (48.42%).

Spatio-Temporal Changes in LULC from 2002 to 2022:

Over the 20-year period from 2002 to 2022, Mardan District experienced significant changes in land use and land cover (LULC) across various categories. This research uses statistical data and geographical maps to illustrate how the landscape evolved, excluding regions that remained unchanged.

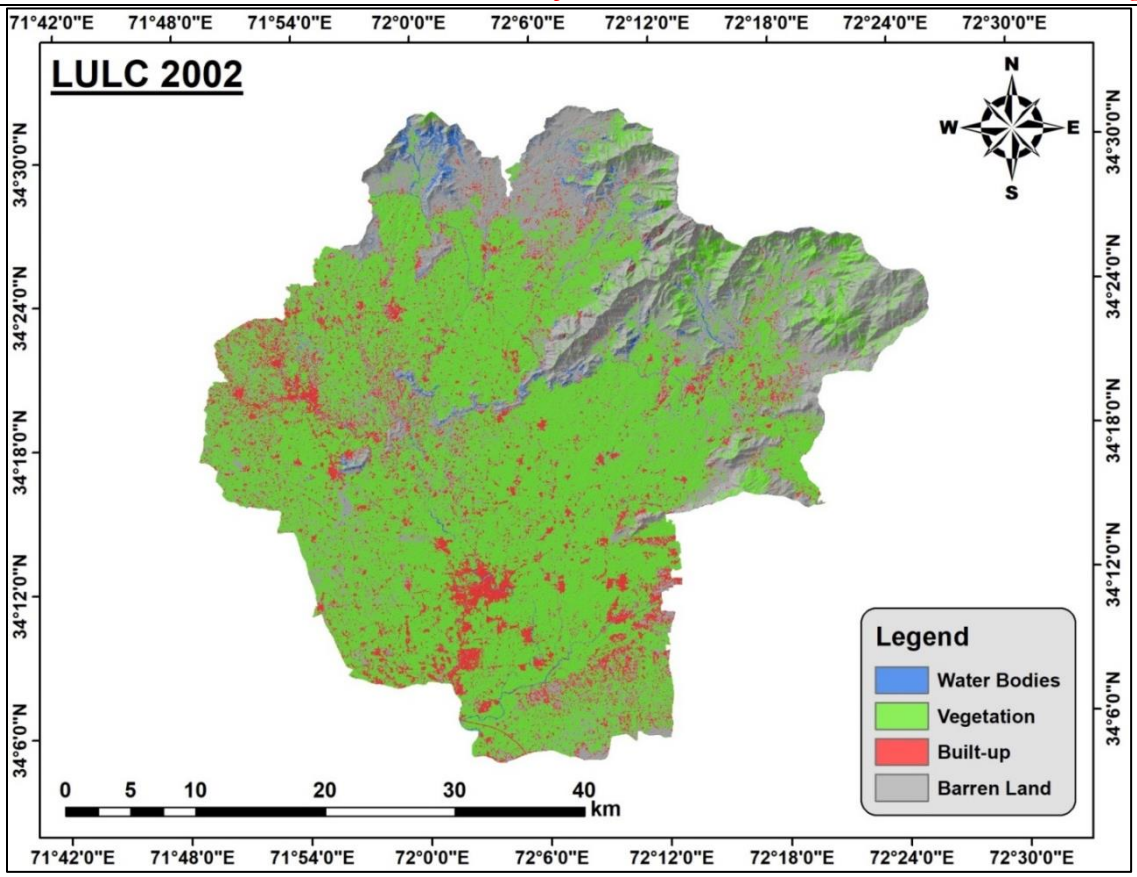

Figure 3: LULC of District Mardan 2002

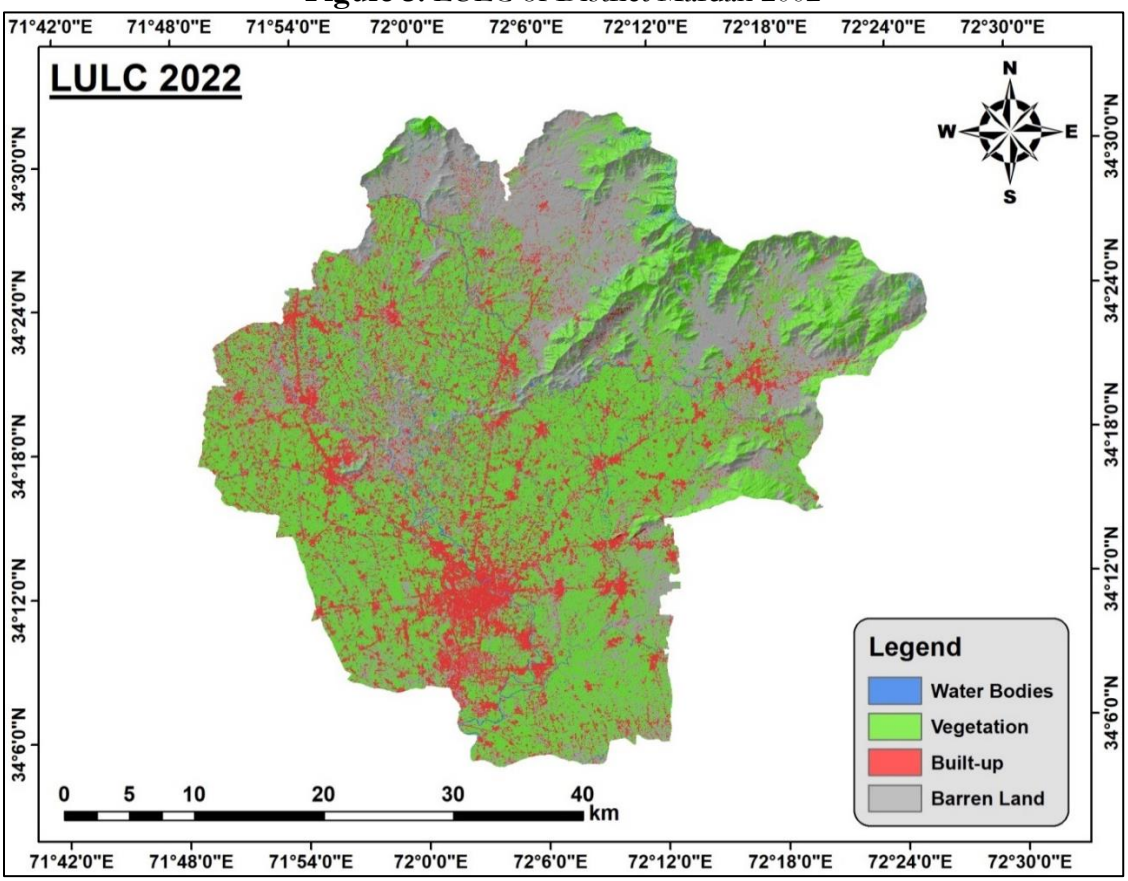

Figure 4: LULC of District Mardan 2022

Table 1: Temporal changes of LULC from 2002 to 2022

LULC	2002		2022	
Classes Names	**Area in Km²**	**%**	**Area in Km²**	**%**
Water Bodies	25.03	1.53	49.61	3.03
Vegetation	928.76	56.71	793.09	48.42
Built-up	165.47	10.10	266.70	16.28
Barren Land	518.60	31.66	528.46	32.27

Barren Land (BA) to Built-up Land (BU):

Approximately 50.70 km², or about 3.10% of the total area, of barren land was converted into built-up land between 2002 and 2022. This transition reflects urban expansion and infrastructure development over the past two decades. The increase in built-up areas, primarily driven by economic growth and population rise, is evident in the orange patches on the map, indicating urbanization of previously unused or sparsely vegetated land.

Barren Land (BA) to Vegetation Land (VG):

Around 177.63 km², or 10.85% of the total area, has transformed from barren land to vegetated land. This change may result from reforestation efforts, agricultural expansion, or natural vegetation restoration. Increasing plant cover is crucial for enhancing ecological balance, boosting biodiversity, and mitigating soil erosion. This shift reflects a growing awareness of the importance of green spaces.

Barren Land (BA) to Water Bodies (WB):

There has been a modest yet noticeable increase in water bodies, covering approximately 12.38 km² (0.76% of the total area). This change could be attributed to new water management projects such as ponds or reservoirs designed to meet irrigation needs and improve water availability. While not as extensive as other changes, these developments are significant for managing the district's water resources.

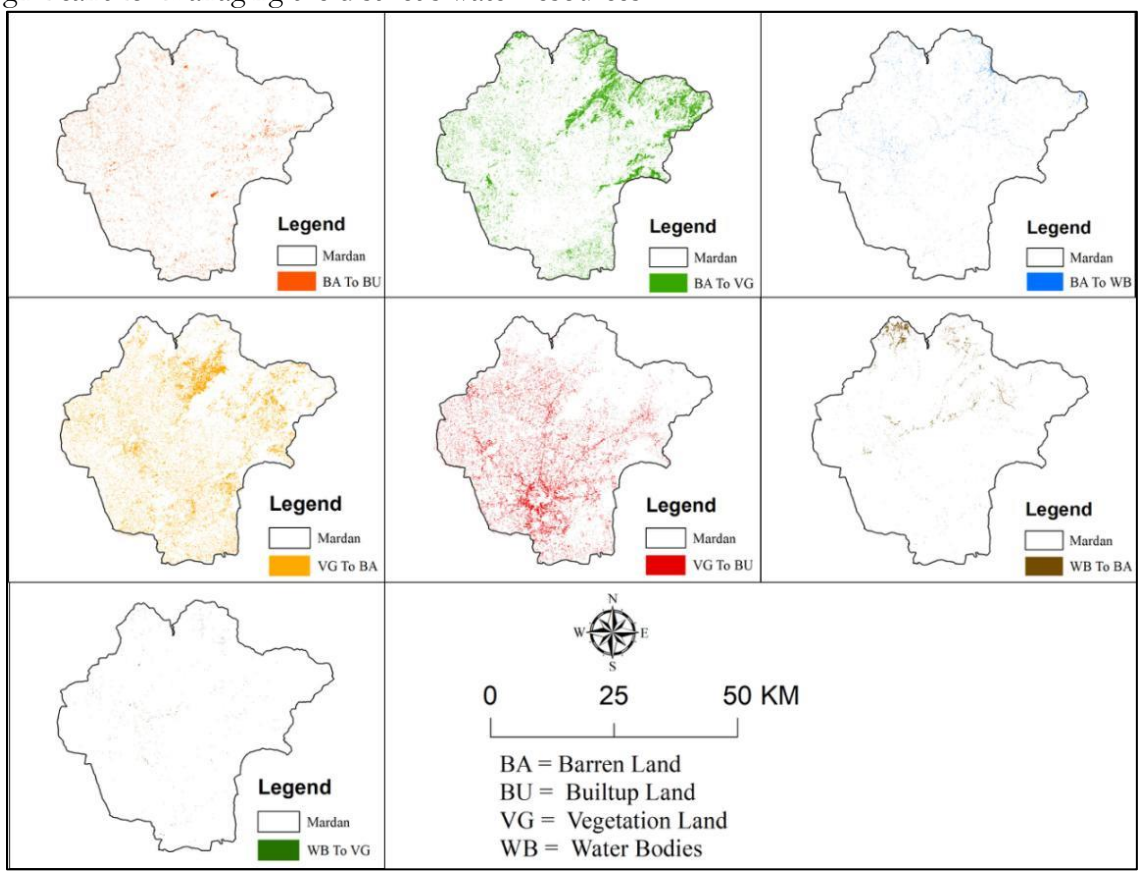

Figure 5: Maps of LULC change from 2002 to 2022

Vegetation Land (VG) to Barren Land (BA):

Conversely, 95.59 km², or 5.84% of the total area, has shifted from vegetated land to barren land. This decline may be due to natural disasters, overgrazing, unsustainable agricultural practices, or deforestation. Addressing these issues requires rehabilitating degraded areas and implementing sustainable land management practices.

Vegetation Land (VG) to Built-up Land (BU):

Areas developed from vegetation, as indicated by red patches on the map, account for approximately 146.16 km² (8.93% of the total area). This trend of converting agricultural or wooded regions into housing and commercial spaces reflects urban sprawl. While indicative of economic growth, it underscores the need for well-planned urban development that balances expansion with environmental preservation.

Water Bodies (WB) to Barren Land (BA):

The conversion of about 1.97 km² of water bodies into barren land, representing 0.12% of the total area, is a minor yet notable change. Possible causes include water depletion, sedimentation, or drying up due to climate change. Preserving existing water bodies is essential for maintaining hydrological balance and supporting local ecosystems.

Water Bodies (WB) to Vegetation Land (VG):

Lastly, the conversion of around 0.96 km², or 0.06% of the total area, from water bodies to vegetation highlights a reduction in water bodies or filling of aquatic areas, leading to vegetation growth. While this shift may benefit native species, it also emphasizes the need to monitor changes in water resource availability.

Table 2: Change in LULC statistics from 2002 to 2022

Class 2002	Class 2022	Change Classes	Change Area Sq.km	Change %
Barren Land	Barren Land	No change	273.17	16.69
Barren Land	Built-up	BA To BU	50.70	3.10
Barren Land	Vegetation	BA To VG	177.63	10.85
Barren Land	Water Bodies	BA To WB	12.38	0.76
Built-up	Built-up	No change	161.23	9.85
Vegetation	Barren Land	VG To BA	189.09	11.55
Vegetation	Built-up	VG To BU	128.82	7.87
Vegetation	Vegetation	No change	620.76	37.92
Water Bodies	Barren Land	WB To BA	15.76	0.96
Water Bodies	Vegetation	WB To VG	2.72	0.17
Water Bodies	Water Bodies	No change	4.60	0.28

Observed LST from 2002 to 2022 using Landsat Data:

Since 2002, Land Surface Temperature (LST) in Mardan District has increased significantly. Figures 6 and 7 show that in 2002, the region's average temperature ranged from 28 to 31 °C and 31 to 33 °C. By 2022, however, the most common temperature ranges shifted to 31–33 °C, 33–35 °C, and 35–41 °C.

In 2002, LST in Mardan District varied from 25°C to 36°C, indicating significant temperature differences across the area. By 2022, this range had expanded dramatically to 20°C to 41°C. This increase highlights the broader range of temperatures and underscores the growing heat, particularly in urban areas.

Figure 7 for 2022 shows that temperature increases have extended towards the borders, affecting a large portion of the city. Approximately one-third of the city experienced temperatures between 31 and 35 °C and 35 to 41 °C. Over time, areas with higher temperatures expanded, while those with lower temperatures diminished. In 2002, most of the region had temperatures between 20 and 28 °C, but by 2022, Mardan City experienced temperatures reaching 35 to 41 °C, reflecting a temperature rise of up to 12 °C over 20 years.

Table 3 provides an overview of LST changes between 2002 and 2022. During this period, the proportion of areas with temperatures between 20 and 23 °C decreased by about 3%. Conversely, the coverage of high LSTs (35–41 °C) increased by 4%, indicating significant surface warming in Mardan City over the past few decades.

Table 3: Temporal trend of LST observed in 2002 & 2022

LST	2002		2022	
Classes Names	**Area in km²**	**%**	**Area in km²**	**%**
20.454 - 28.719	147.94	9.03	100.05	6.11
28.72 - 31.116	466.99	28.51	360.95	22.05
31.117 - 33.182	511.98	31.26	493.15	30.13
33.183 - 35.58	362.40	22.13	426.59	26.06
35.581 - 41.531	148.54	9.07	256.14	15.65

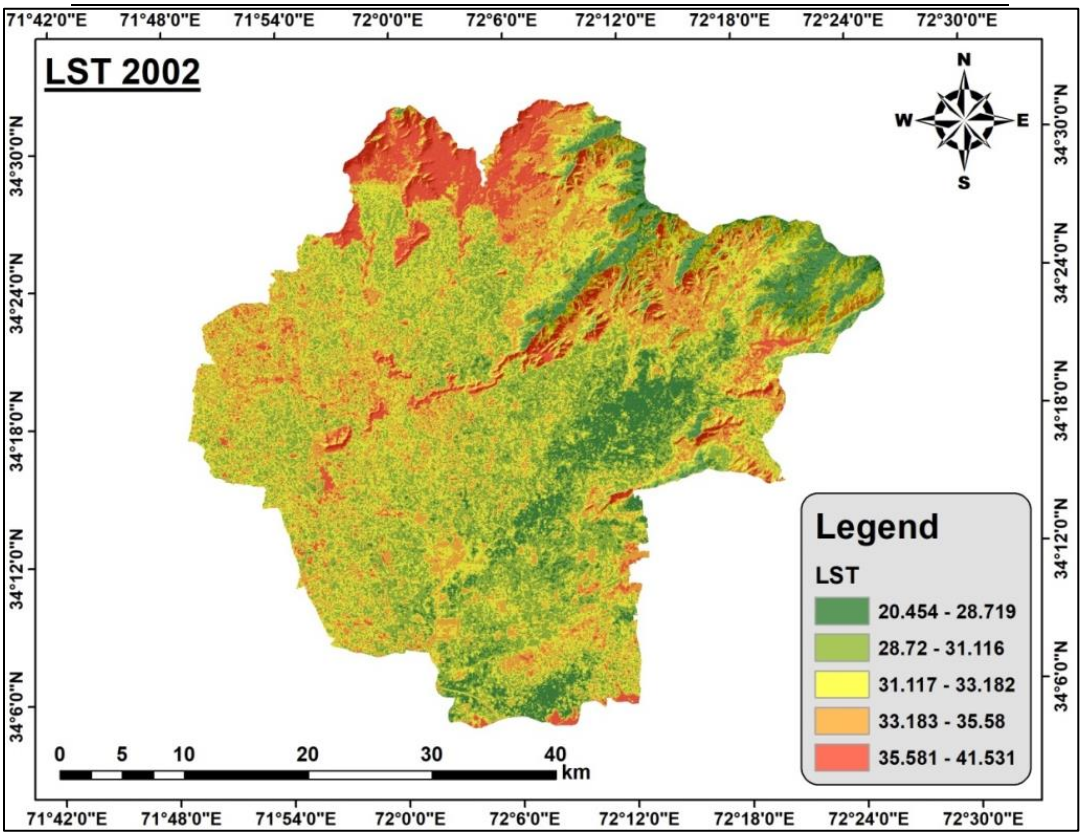

Figure 6: LST Map of 2002

Spatio-Temporal Changes in LST from 2002 to 2022:

The examination of Land Surface Temperature (LST) changes in District Mardan, Khyber Pakhtunkhwa, from 2002 to 2022 reveals significant shifts between various temperature classes. Understanding these geographical and temporal dynamics is crucial for effective environmental management and policymaking.

Spatio-Temporal Changes in Land Surface Temperature (LST) from 2002 to 2022:

District Mardan's Land Surface Temperature (LST) data shows a general upward trend from 2002 to 2022. This trend is particularly evident with large areas shifting from "Very Low" (VL) and "Low" (L) temperature classes to "Medium" (M), "High" (H), and "Very High" (VH). Overall, approximately 519.70 km² of the region transitioned from colder to warmer temperature classes. Conversely, around 218.49 km² experienced cooling, shifting to colder classes. This net rise in temperatures over the 20-year period is attributed to urbanization, land use changes, and other human-induced factors. Detailed transitions of LST classes are as follows:

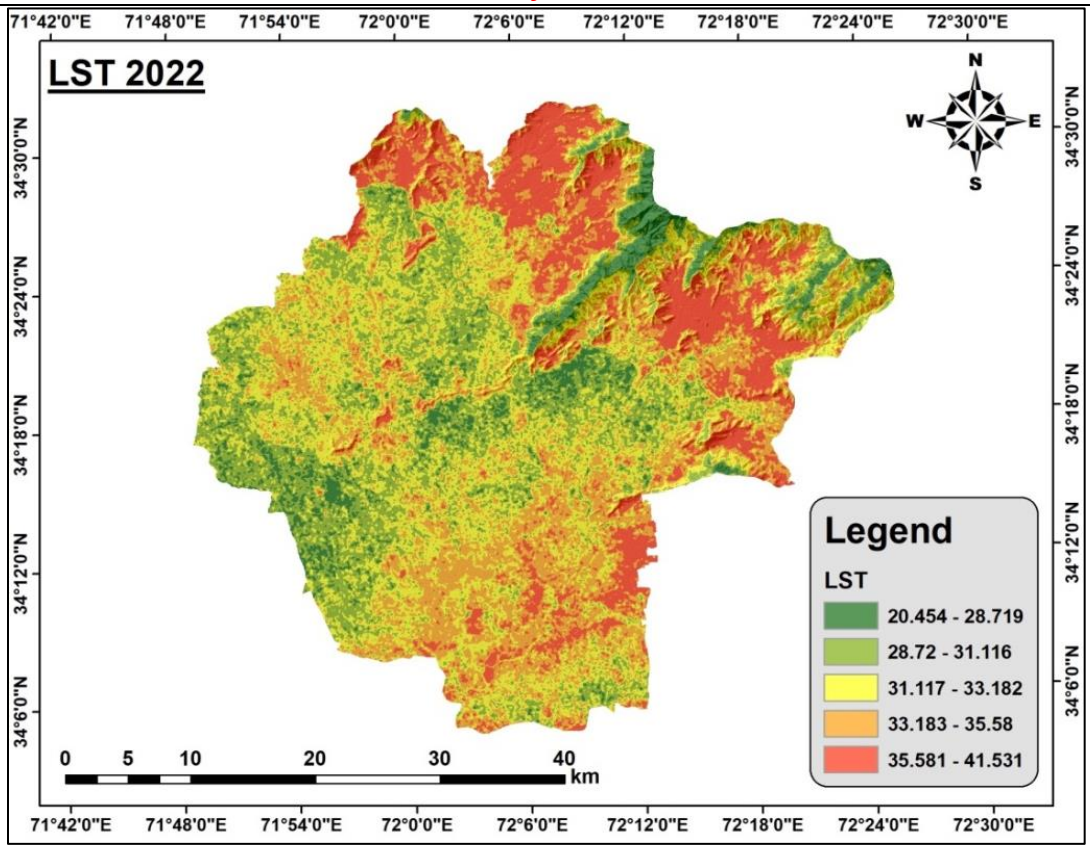

Figure 7: LST Map of 2022

Very Low LST Class to Other LST Classes:

The "Very Low" (VL) temperature class showed minimal change, with 37.10 km² (2.27% of the total area) remaining in this category. Significant shifts from VL to higher temperature classes indicate growing heat spots. Specifically, 40.94 km² (2.50% of the total area) shifted from VL to "Low" (L), 37.39 km² (2.28%) transitioned to "Medium" (M), 25.44 km² (1.55%) moved to "High" (H), and 6.04 km² (0.37%) shifted to "Very High" (VH). These increases highlight areas of rapid warming, likely due to urbanization, deforestation, or land use changes.

Low LST Class to Other LST Classes:

The "Low" (L) temperature class exhibited various transitions:

- 28.32 km² (1.73%) moved from Low to Very Low, suggesting cooling possibly due to reforestation or reduced human activity.
- 129.69 km² (7.92%) remained in the Low class, indicating stable temperatures.
- 172.25 km² (10.52%) shifted from Low to Medium, reflecting moderate warming due to urbanization or agriculture.
- 107.25 km² (6.55%) transitioned from Low to High, indicating significant warming likely from new infrastructure.
- 30.44 km² (1.86%) moved from Low to Very High, highlighting regions with sharp temperature increases due to widespread land use changes.

Moderate LST Class to Other LST Classes:

The "Moderate" (M) temperature class showed both increases and decreases in temperature:

- 21.06 km² (1.29%) cooled from M to Very Low, possibly due to effective land management.
- 133.53 km² (8.16%) transitioned from M to Low, indicating a slight cooling trend.

- 180.15 km² (11.01%) remained in the M class, suggesting minimal temperature fluctuation.
- 131.41 km² (8.03%) shifted from M to High, reflecting significant warming likely due to industrialization and urbanization.
- 48.22 km² (2.95%) moved from M to Very High, indicating regions with extremely high temperatures, possibly due to increased human activity and environmental degradation.

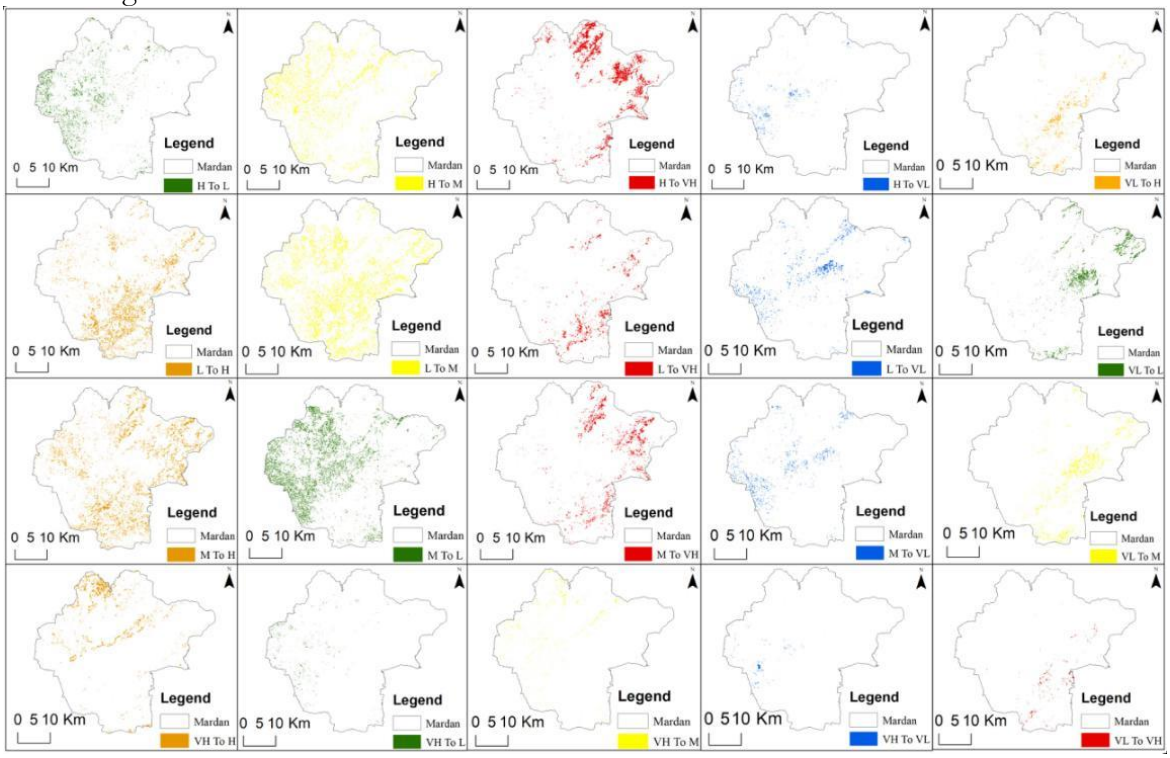

Figure 8: LST Changes in Classes from 2002 – 2022

High LST Class to Other LST Classes:

The "High" (H) temperature class transitions indicate notable environmental changes:

- 9.75 km² (0.60%) cooled from High to Very Low, suggesting effective temperature reduction in some areas.
- 50.90 km² (3.11%) shifted from High to Low, indicating slight cooling.
- 92.68 km² (5.66%) transitioned from High to Moderate, showing minor temperature decreases, potentially due to improved land management or conservation efforts.
- 118.63 km² (7.25%) remained in the High class, indicating minimal temperature change.
- 88.94 km² (5.43%) moved from High to Very High, reflecting significant warming likely due to increased urbanization and land use changes.

Very High LST Class to Other LST Classes:

Changes in the "Very High" (VH) temperature class provide insight into the most impacted areas:

- 3.03 km² (0.19%) cooled significantly from VH to Very Low, likely due to effective environmental restoration.
- 6.13 km² (0.37%) transitioned from VH to Low, indicating some cooling trends.
- 11.89 km² (0.73%) shifted from VH to Moderate, showing mild cooling.
- 43.85 km² (2.68%) moved from VH to High, indicating minor cooling while still remaining in higher temperature categories.

- 81.82 km² (5.00%) remained in the Very High class, showing minimal change in the highest temperature category.

Table 4: LST Changes in Classes from 2002 - 2022

Class 2002	Class 2022	Change Classes	Change Area Sq Km	Change %
VL	VL	VL To VL	37.10	2.27
VL	L	VL To L	40.94	2.50
VL	M	VL To M	37.39	2.28
VL	H	VL To H	25.44	1.55
VL	VH	VL To VH	6.04	0.37
L	VL	L To VL	28.32	1.73
L	L	L To L	129.69	7.92
L	M	L To M	172.25	10.52
L	H	L To H	107.25	6.55
L	VH	L To VH	30.44	1.86
M	VL	M To VL	21.06	1.29
M	L	M To L	133.53	8.16
M	M	M To M	180.15	11.01
M	H	M To H	131.41	8.03
M	VH	M To VH	48.22	2.95
H	VL	H To VL	9.75	0.60
H	L	H To L	50.90	3.11
H	M	H To M	92.68	5.66
H	H	H To H	118.63	7.25
H	VH	H To VH	88.94	5.43
VH	VL	VH To VL	3.03	0.19
VH	L	VH To L	6.13	0.37
VH	M	VH To M	11.89	0.73
VH	H	VH To H	43.85	2.68
VH	VH	VH To VH	81.82	5.00

Measurement of Coefficient of Determination for LST with Normalized Satellite Indices:

Table 5 presents the annual fluctuations in Land Surface Temperature (LST) for Mardan region in 2002 and 2022, based on various normalized satellite indices. The data reveals a significant increase in the annual variability of LST over the past two decades. This fluctuation is particularly evident when compared to indices such as the Normalized Difference Built-up Index (NDBI), Soil Adjusted Vegetation Index (SAVI), Normalized Difference Vegetation Index (NDVI), and Bare Soil Index (BI).

From 2002 to 2022, LST showed a statistically significant positive correlation with SAVI, NDBI, and BI, particularly in Mardan City. This suggests that as urbanization and soil exposure increased, so did LST, leading to higher temperatures in less vegetated and more built-up areas. Conversely, a negative correlation was observed between LST and NDVI and NDWI, indicating that cooler temperatures were associated with areas of higher vegetation and water bodies. This pattern underscores the role of greenery and water in mitigating urban heat.

Unfavorable trends in LST have been noted in Mardan's western and elevated regions, where the absence of vegetation has significantly raised temperatures. In contrast, a small area in Mardan's eastern and lower regions exhibited an inverse association with NDVI, complicating the assessment of LST patterns due to sparse vegetation. Overall, the strong

correlation between LST and the various indices assessed annually highlights the complex relationship between surface temperatures, vegetation cover, and urban expansion. By 2022, the positive correlation between LST and these indicators had risen by 75.4%, underscoring the significant impact of environmental variables and urbanization on temperature fluctuations in Mardan.

LST and NDVI:

2002: There is a substantial negative correlation (R^2 = -0.6530) between LST and NDVI, indicating that lower LST levels are associated with higher NDVI values, which reflect denser vegetation. This suggests that vegetation effectively contributes to surface cooling.

2022: The negative association persists but is weaker, with the correlation dropping to -0.5453. This indicates a reduced cooling effect of vegetation, possibly due to urban expansion reducing green spaces.

LST and NDWI:

2002: There is a moderate positive correlation (R^2 = 0.4140) between LST and NDWI. This is somewhat unexpected since water bodies typically have a cooling effect. The positive association might be due to urban heat islands near water bodies, which could contribute to higher temperatures.

2022: The correlation weakens to 0.2142, reflecting a slight positive link. This change may result from altered land use practices around water bodies or specific meteorological conditions during the study period.

LST and SAVI:

2002: There is a strong negative correlation (R^2 = -0.7250) between LST and SAVI, indicating that lower LST is associated with higher SAVI values, which suggest better vegetation with less soil influence.

2022: The correlation weakens significantly to 0.1354, showing a very weak positive link. This suggests a decreased role of soil-adjusted vegetation in cooling the land surface, potentially due to increased urbanization and reduced green space.

LST and NDBI:

2002: There is a very strong positive correlation (R^2 = 0.8910) between LST and NDBI, indicating that higher LST is associated with higher NDBI values, which reflect more built-up areas. This shows that urban areas significantly raise land surface temperatures.

2022: The correlation increases to 0.9927, further strengthening the association. This suggests that built-up areas are contributing even more to higher temperatures, reflecting an intensification of the urban heat island effect.

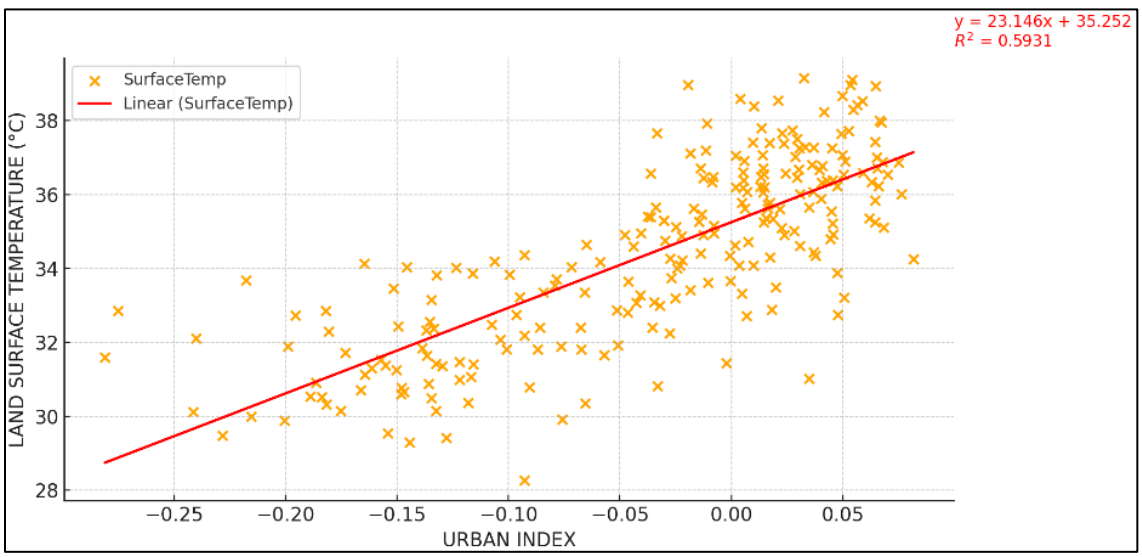

Figure 9: Linear Regression Model LST and UI

LST and BI:

2002: There is a strong positive correlation (R^2 = 0.7580) between LST and BI, indicating that higher LST is associated with higher BI values, which denote more bare soil. This suggests that bare soil may contribute to rising temperatures.

2022: The correlation decreases to 0.6564, indicating a moderate positive link. This suggests that while bare soil still impacts LST, other factors such as increased urbanization or changes in land use may have reduced its influence.

Table 5: LST with Normalized Indices

Years	Indices	LST	NDVI	NDWI	SAVI	NDBI	BI
2002	LST	1.0000	-0.6530	0.4140	-0.7250	0.5931	0.7580
	NDVI	-0.7320	1.0000	-0.7841	0.9085	-0.8671	-0.8282
	NDWI	0.6321	-0.7746	1.0000	0.8510	-0.8157	-0.7819
	SAVI	-0.7203	0.9078	-0.8487	1.0000	-0.8813	-0.9265
	NDBI	0.8871	-0.8656	0.6555	-0.9288	1.0000	0.9477
	BI	0.7510	-0.8281	0.5979	-0.9228	0.9918	1.0000
2022	LST	1.0000	−0.5453	0.2142	0.1354	0.6672	0.6564
	NDVI	−0.5453	1.0000	−0.7087	1.0000	−0.7791	−0.8248
	NDWI	−0.1609	−0.7087	1.0000	−0.7214	0.1481	0.8252
	SAVI	0.7354	1.0000	−0.7214	1.0000	−0.7698	0.4390
	NDBI	0.9927	−0.7791	0.1481	−0.7798	1.0000	0.6073
	BI	0.7564	−0.8248	0.8252	0.3247	0.2633	1.0000

Calculation of LST from Urban Indices:

The linear regression model used to forecast Land Surface Temperature (LST) based on urban indices (UI) is illustrated in Figure 9. The model reveals a strong relationship between LST and UI, with an R^2 value of 0.89, indicating a significant correlation. This robust connection suggests that, despite potential saturation issues commonly affecting indices like NDVI, the relationship between LST and UI remains substantial. As UI increases, temperatures are positively correlated, reflecting a consistent trend of rising temperatures associated with urban growth.

Using Landsat data from 2022, the linear regression model was validated and confirmed to align well with established temperature trends. The model compared temperatures derived from the model (Tmod) with those observed from the satellite (Tsat). This analysis, based on data from 300 locations within the study area, utilized Landsat 8 thermal data and UI temperature readings, as shown in Figure 9. The model's accuracy in predicting temperature fluctuations was effectively validated through this comparison.

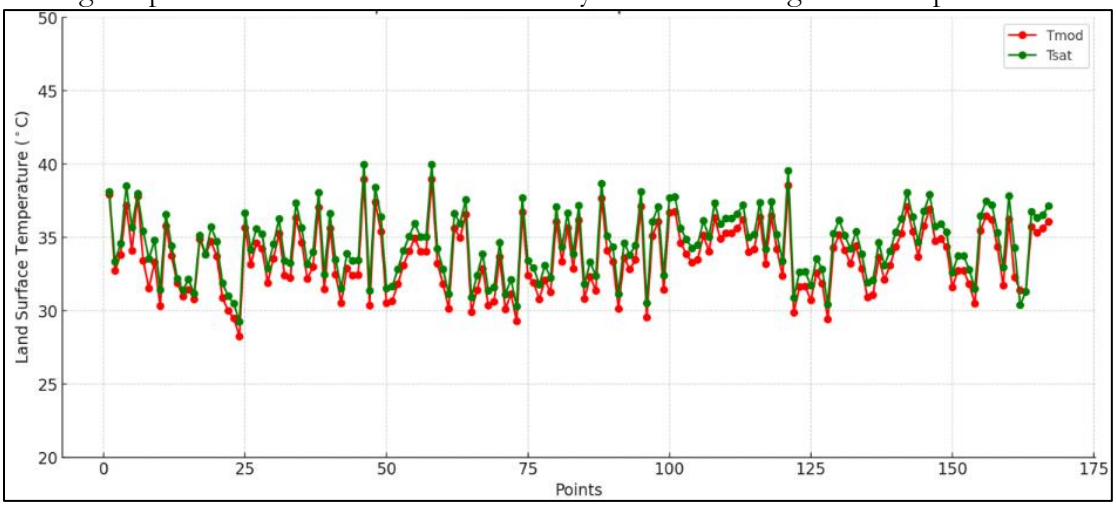

Figure 10: Comparisons between TMOD and TSAT

Discussion:

To anticipate land use, land cover, and Land Surface Temperature (LST) in Mardan, Khyber Pakhtunkhwa, Pakistan, this study employed Markov chain models combined with cellular automata. The effectiveness of various land cover indices in forecasting temperature changes over time was assessed. Among the indices examined—including the Soil-Adjusted Vegetation Index (SAVI), Normalized Difference Vegetation Index (NDVI), Normalized Difference Built-up Index (NDBI), and Built-up Index (BI)—the Normalized Difference Water Index (NDWI) proved to be the most accurate predictor of LST distribution. Linear regression techniques were used to predict the development of city centers and surrounding temperatures. Multiple linear regressions were suitable as long as there was no direct relationship between the predicted variables. Considering the interdependence of various factors, the Urban Index (UI) emerged as the most reliable temperature predictor. The UI model was used to estimate the potential environmental impacts of LST by predicting urban growth and future temperature trajectories. The model forecasted temperatures with an average absolute error of 1.83 °C, based on thermal band LST data and linear regression incorporating UI. Recent studies confirm a strong correlation between UI's heat forecasts and urban expansion metrics.

Although previous research had not established the link between temperature and UI, this study demonstrates that higher temperatures in areas with more built-up structures and less vegetation are indicative of UI's predictive strength. Comparable urban indices are observed in water-intensive and residential regions of Colombo, Sri Lanka. The high correlation between UI and LST aligns with research showing that urban climate intensity significantly impacts residential water and energy use. In addition, the Support Vector Machine (SVM) classifier was evaluated for high-accuracy classification of urban land use and land cover (LULC) distribution for the years 1990 and 2018. The SVM classifier produced highly accurate maps, exceeding the necessary 80% accuracy level, by using digitized areas rather than points for classification. The findings of this study are crucial for informing urban planning and management in Khyber Pakhtunkhwa. They will enhance the district's approach to issues such as land record management, solid waste management infrastructure, capacity building, landfill development, pond removal, and support for local governments in rehabilitating unsafe buildings.

Conclusion:

Significant changes driven by urbanization are evident from the spatiotemporal analysis of Land Use and Land Cover (LULC) in Mardan from 2002 to 2022. The study reveals a notable increase in built-up areas, which rose from 165.47 km² to 266.70 km², at the expense of vegetative and agricultural land. Concurrently, vegetation decreased from 928.76 km² to 793.09 km², highlighting the ongoing trade-off between urban expansion and natural land cover. The overall accuracy (OA) improved from 81% in 2002 to 87% in 2022, validating the reliability of the study's Maximum Likelihood Classification (MLC) algorithm. This increase underscores the accuracy of the classification and emphasizes the impact of urbanization on the environment, evidenced by the reduction in vegetative cover and the expansion of arid and built-up areas.

Additionally, Land Surface Temperature (LST) data show a discernible trend of rising temperatures over the past 20 years. The average LST range shifted from 25–36°C in 2002 to 20–41°C in 2022, with higher temperatures becoming more common. The positive correlation between LST and urban indices (UI) indicates a direct link between the growth of built-up areas and the reduction in vegetative cover, exacerbating temperature increases. This study highlights the importance of integrating green spaces and water bodies into urban development plans to balance growth with environmental sustainability. The findings offer valuable insights into the dynamic changes in land use and temperature in Mardan, providing

policymakers with crucial information to enhance urban sustainability and resilience in the face of ongoing development and climate challenges.

Recommendations:

Land use and land cover change (LULC) is a significant driver of global change, affecting climate, ecosystem processes, biogeochemical cycles, biodiversity, and human activities. To alleviate pressure on agricultural lands, the government should prioritize selecting unproductive and infertile lands for housing projects. Agricultural lands are crucial for producing ecological goods and services such as clean air, clean water, and sustainable habitats. Vegetation plays a vital role in the global climate system by regulating energy distribution over large portions of the land surface. According to regulations, fertile and primary agricultural land should only be used for agricultural purposes. The conversion of agricultural and cultivable lands into housing developments poses a major challenge. Therefore, legislation is needed to protect agricultural lands from unauthorized housing projects. The government must enact laws to prevent the conversion of agricultural lands and ensure that relevant organizations enforce these regulations.

In District Mardan, vegetation has decreased from 56% to 48%. To counter this, the government should prioritize plantation and afforestation efforts, as plants help reduce temperatures by absorbing harmful gases and blocking radiation from reaching the Earth's surface. Urban sprawl significantly contributes to rising temperatures, as built-up areas absorb more radiation than they emit, resulting in higher and more prolonged surface temperatures. Urban areas in Mardan have increased by 6%, highlighting the need for stricter control over unplanned urbanization to mitigate environmental and climatic impacts. Additionally, barren land in the district has increased by 1%. Improving the canal system could help convert barren land into productive vegetation, further benefiting the environment.

References:

[1] G. X. Zhao, G. Lin, and T. Warner, "Using Thematic Mapper data for change detection and sustainable use of cultivated land: a case study in the Yellow River delta, China," Int. J. Remote Sens., vol. 25, no. 13, pp. 2509–2522, Jul. 2004, doi: 10.1080/01431160310001619571.

[2] V. N. Mishra, R. Prasad, P. Kumar, D. K. Gupta, S. Agarwal, and A. Gangwal, "Assessment of Spatio-Temporal Changes in Land Use/Land Cover Over a Decade (2000–2014) Using Earth Observation Datasets: A Case Study of Varanasi District, India," Iran. J. Sci. Technol. - Trans. Civ. Eng., vol. 43, no. 1, pp. 383–401, Jul. 2019, doi: 10.1007/S40996-018-0172-6/METRICS.

[3] M. M. H. Seyam, M. R. Haque, and M. M. Rahman, "Identifying the land use land cover (LULC) changes using remote sensing and GIS approach: A case study at Bhaluka in Mymensingh, Bangladesh," Case Stud. Chem. Environ. Eng., vol. 7, p. 100293, Jun. 2023, doi: 10.1016/J.CSCEE.2022.100293.

[4] T. K. Rudel, "Land Use and Land Use Change," Handbooks Sociol. Soc. Res., pp. 425–438, 2021, doi: 10.1007/978-3-030-77712-8_20.

[5] C. Liping, S. Yujun, and S. Saeed, "Monitoring and predicting land use and land cover changes using remote sensing and GIS techniques—A case study of a hilly area, Jiangle, China," PLoS One, vol. 13, no. 7, p. e0200493, Jul. 2018, doi: 10.1371/JOURNAL.PONE.0200493.

[6] H. Landsberg, "The Urban Climate, Volume 28 - 1st Edition," Urban Clim., p. 275, 1981, Accessed: Jul. 18, 2024. [Online]. Available: https://www.elsevier.com/books/the-urban-climate/landsberg/978-0-12-435960-4

[7] B. Ackerman, "Temporal March of the Chicago Heat Island," J. Appl. Meteorol. Climatol., vol. 24, no. 6, pp. 547–554, Jun. 1985, doi: 10.1175/1520-0450(1985)024.

[8] X. L. Chen, H. M. Zhao, P. X. Li, and Z. Y. Yin, "Remote sensing image-based

analysis of the relationship between urban heat island and land use/cover changes," Remote Sens. Environ., vol. 104, no. 2, pp. 133–146, Sep. 2006, doi: 10.1016/J.RSE.2005.11.016.

[9] P. N. Haindongo, A. M. Kalumba, and I. R. Orimoloye, "Local people's perceptions about Land Use Cover Change (LULCC) for sustainable human wellbeing in Namibia," GeoJournal, vol. 87, no. 3, pp. 1727–1741, Jun. 2022, doi: 10.1007/S10708-020-10337-7/METRICS.

[10] T. Bibi, F. Nawaz, A. Abdul Rahman, and A. Latif, "FLOOD HAZARD ASSESSMENT USING PARTICIPATORY APPROACH AND WEIGHTED OVERLAY METHODS," Int. Arch. Photogramm. Remote Sens. Spat. Inf. Sci., vol. XLII-4-W16, no. 4/W16, pp. 153–160, Oct. 2019, doi: 10.5194/ISPRS-ARCHIVES-XLII-4-W16-153-2019.

[11] D. R. Streutker, "A remote sensing study of the urban heat island of Houston, Texas," Int. J. Remote Sens., vol. 23, no. 13, pp. 2595–2608, Jul. 2002, doi: 10.1080/01431160110115023.

[12] Z. Hassan et al., "Dynamics of land use and land cover change (LULCC) using geospatial techniques: a case study of Islamabad Pakistan," Springerplus, vol. 5, no. 1, pp. 1–11, Dec. 2016, doi: 10.1186/S40064-016-2414-Z/FIGURES/6.

[13] C. C. Burt, "The World's Hottest Recorded Air Temperatures," Weather. POWER, BEAUTY, Excit., vol. 64, no. 2, pp. 26–33, Jan. 2011, doi: 10.1080/00431672.2011.551594.

[14] E. López, G. Bocco, M. Mendoza, and E. Duhau, "Predicting land-cover and land-use change in the urban fringe: A case in Morelia city, Mexico," Landsc. Urban Plan., vol. 55, no. 4, pp. 271–285, Aug. 2001, doi: 10.1016/S0169-2046(01)00160-8.

[15] F. Fan, Y. Wang, and Z. Wang, "Temporal and spatial change detecting (1998-2003) and predicting of land use and land cover in Core corridor of Pearl River Delta (China) by using TM and ETM+ images," Environ. Monit. Assess., vol. 137, no. 1–3, pp. 127–147, Jun. 2008, doi: 10.1007/S10661-007-9734-Y/METRICS.

[16] A. Tariq and H. Shu, "CA-Markov Chain Analysis of Seasonal Land Surface Temperature and Land Use Land Cover Change Using Optical Multi-Temporal Satellite Data of Faisalabad, Pakistan," Remote Sens. 2020, Vol. 12, Page 3402, vol. 12, no. 20, p. 3402, Oct. 2020, doi: 10.3390/RS12203402.

[17] A. Tariq, J. Yan, and F. Mumtaz, "Land change modeler and CA-Markov chain analysis for land use land cover change using satellite data of Peshawar, Pakistan," Phys. Chem. Earth, Parts A/B/C, vol. 128, p. 103286, Dec. 2022, doi: 10.1016/J.PCE.2022.103286.